2.1. Analyses of structures under fire

L. Kwasniewski
Warsaw University of Technology, Poland

D. Bacinskas, E. Geda, V. Gribniak & G. Kaklauskas
Vilnius Gediminas Technical University, Lithuania

G. Cefarelli, B. Faggiano, A. Ferraro, F.M. Mazzolani & E. Nigro
University of Napoli "Federico II", Italy

C. Couto, N. Lopes & P. Vila Real
University of Aveiro, Portugal

M. Hajpál & Á. Török
Budapest University of Technology and Economics, Hungary

M. Kaliske
University of Leipzig, Germany

D. Pintea & R. Zaharia
University of Timisoara, Romania

2.1.1. INTRODUCTION

The main objective of a fire-structure analysis is to predict the effects of fires in buildings, e.g. the fire resistance and the structure's performance under heating and cooling caused by fire. The results of such analysis can be applied in the design of fire protection systems, in the evaluation of fire safety and as an addendum of experiments. Advanced calculation techniques can be helpful in the areas where experiments encounter difficulties such as testing large specimens, implementation of loading and boundary condition, measurements and interpretation of specimen's behaviour.

A computational model used for fire-structural (member or global) analysis should properly represent the considered problem in terms of: type of analysis and solution methods, geometry, temperature dependent material properties, mechanical boundary conditions and loading, thermal conditions.

The fire resistance analysis of reinforced concrete (RC) structures faces additional challenges and constitutes an important part in their design. From the constructional point of view, buildings and structures at fire have to carry mechanical loadings and thus provide safe people evacuation (rescue) and safe firemen work. High temperatures have a very significant adverse effect on thermo-mechanical properties of RC members. High temperature substantially reduces strength of concrete and steel, and causes significant increase in cracking, strains and deflections. Load bearing capacity of structure decreases and may fail at critical points.

2.1.2 TYPE OF ANALYSIS AND SOLUTION METHODS

Depending on the simulated test scenario, three types of analysis can be considered: structural, thermal or coupled structural-thermal. Structural stress analysis should be able to take into account strains due to elastic and plastic deformation and due to thermal elongation if coupled structural-thermal analysis is performed. Creep strains can usually be omitted for transient analysis. Incremental, transient structural analysis should be based on explicit or implicit methods for time integration. Application of explicit methods in coupled structural-thermal fire analysis is not feasible due to consideration of relatively long time intervals. For the thermal calculations usually unconditionally stable implicit time integration is applied (Hallquist 2006).

One can choose between general purpose commercial programs and research oriented specialized unique programs developed by academia. In both cases, the majority of today's computer programs, dedicated to structural analysis, are based on the Finite Element (FE) Method.

Well validated nonlinear codes are preferred over specialized, experimental computer programs. A chosen code should cover all analysis aspects, important for the considered case.

2.1.3 THERMAL PROPERTIES OF MATERIALS

In fire conditions the temperature dependent properties shall be taken into account. The thermal and mechanical properties of steel, concrete, aluminium should be determined from the following clauses.

2.1.3.1 Steel

The relative thermal elongation of steel $\Delta l/l$ is given in formulae (2.1.3.1 a-c) from EN-1993-1-2). In these formulae the thermal elongation of steel is computed as function of the steel temperature θ_a. EN 1993-1-2 gives formulae (2.13.2 a-d) for computing the specific heat of steel c_a as function of the steel temperature θ_a. The thermal conductivity of steel λ_a is given by the formulae (3.3 a-b) as function of the steel temperature θ_a. The graphical representation of these formulae is also given for each of the thermal properties.

The thermal conductivity of steel as function of the temperature is presented in Figure 2.1.1.

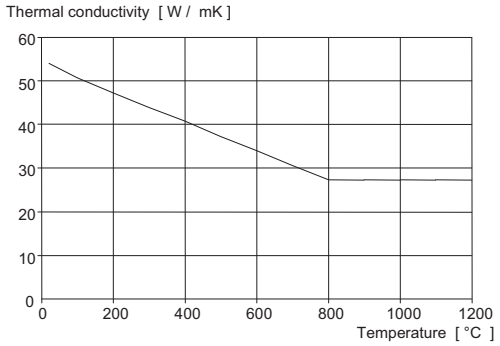

Figure 2.1.1. Thermal conductivity of steel at elevated temperature.

2.1.3.2 Aluminium alloys

The formulae for computing the relative thermal elongation (strain) of aluminium alloys $\Delta l/l$ are given in paragraph "3.3.1.1 Thermal elongation" from EN 1999-1-2 as function of the aluminium temperature θ_{al}. The formulae for computing the specific heat of aluminium c_{al} as function of the aluminium temperature are given in paragraph "3.3.1.2 Specific heat". The variation of the specific heat of the aluminium alloys with the temperature is presented in Figure 2.1.2. Similarly the computation of the thermal conductivity of aluminium alloys as function of the aluminium temperature is given in paragraph "3.3.1.3 Thermal conductivity".

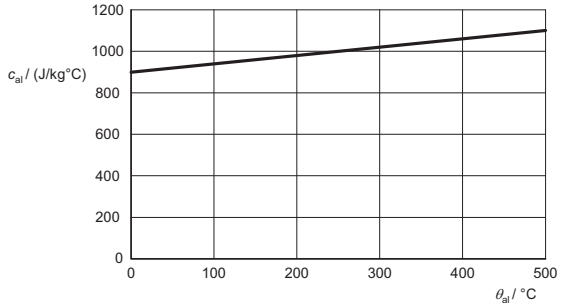

Figure 2.1.2. Specific heat of aluminium alloys as a function of the temperature.

2.1.3.3 Concrete with siliceous and calcareous aggregates

The thermal strain of concrete $\varepsilon_c(\theta)$ is given in formulae as function of concrete temperature for siliceous and calcareous aggregates in paragraph "3.3.1 Thermal elongation, see EN 1992-1-2. The formulae for computing the specific heat $c_p(\theta)$ of dry concrete (u=0%) with siliceous and calcareous aggregates is given in paragraph "3.3.2 Specific heat" (EN 1992-1-2) as function of the concrete temperature. Where the moisture content is not considered explicitly in the calculation method, the function given for the specific heat of concrete with siliceous or calcareous aggregates may be modelled by a constant value, $c_{p.peak}$, situated between 100°C and 115°C with linear decrease between 115°C and 200°C.

The thermal conductivity λ_c of concrete may be determined between lower and upper limit values, given in paragraph "3.3.3 Thermal conductivity" as function of the concrete temperature. The thermal conductivity of concrete is presented in Figure 2.1.3.

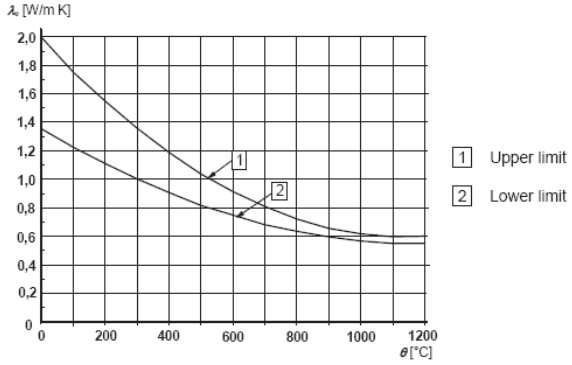

Figure 2.1.3. Thermal conductivity of concrete.

2.1.1.4 Natural stones

The heating causes a colour change of stones, see Figure 2.1.4a. Not only colour but also other external signs of heat are observed. Limestone samples are cracked at lower temperatures while at higher temperature the samples collapsed or exploded, see Figure 2.1.4b. According to the thermal decomposition of carbonates this processes is dedicated to the formation of new mineral phases (portlandite).

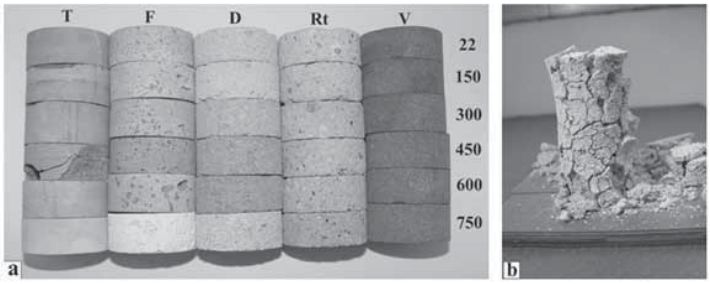

Figure 2.1.4. a) Visible colour changes of different stone types before heating and after heating from 150°C to 750°C. T-Tardos compact limestone, F-Süttő travertine, D-Sóskút coarse limestone, Rt-Egertihamér rhyolite tuff, V-Balatonrendesi sandstone, b) Crack formation nad disintegration of cylindrical sample of Sóskút coarse limestone sample. after heating on 900°C (after Hajpál 2008).

Figure 2.1.5. a) Scaling at window edges in Lobenfeld b) Rounding of edges in Dresden.

The most important kind of decay of stones due to fire are scaling off, see Figure 2.1.5a, spalling, cracking, rounding off the edges, see Figure 2.1.5b. Fire can completely destroy ornaments and can damage carved forms. Fire damaged stones are often replaced by new ones (Hajpál 2000).

2.1.4 MECHANICAL PROPERTIES OF STRUCTURAL ELEMENTS

2.1.4.1 Carbon steel

For heating rates between 2 and 50 K/min, the strength and deformation properties of structural steel at elevated temperatures should be obtained from the stress-strain relationship given in Figure 2.1.6. Table 2.1.3.1 (EN1993-1-2) gives the reduction factors for the stress-strain relationship for steel at elevated temperatures. These reduction factors are defined as follows:

effective yield strength, relative to yield strength at 20 °C:

$$k_{y,\theta} = f_{y,\theta} / f_y$$

proportional limit, relative to yield strength at 20 °C: $k_{p,\theta} = f_{p,\theta} / f_y$

slope of linear elastic range, relative to slope at 20 °C:

$$k_{E,\theta} = E_{a,\theta} / E_a$$

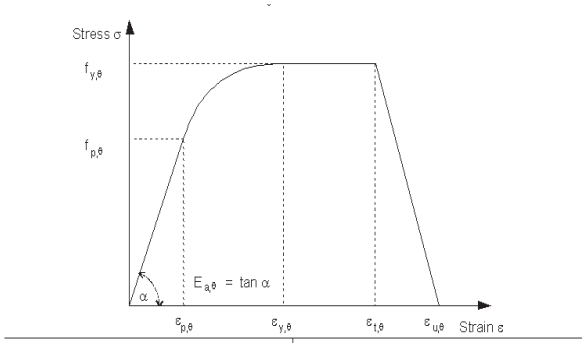

$f_{y,\theta}$	effective yield strength;	$\varepsilon_{p,\theta}$	strain at the proportional limit;
$f_{p,\theta}$	proportional limit;	$\varepsilon_{y,\theta}$	yield strain;
$E_{a,\theta}$	slope of the linear elastic range;	$\varepsilon_{t,\theta}$	limiting strain for yield strength;
		$\varepsilon_{u,\theta}$	ultimate strain.

Figure 2.1.6. Stress-strain relationship for carbon steel at elevated temperatures.

2.1.4.2 Aluminium alloys

For thermal exposure up to 2 hours, the 0,2 % proof strength at elevated temperature of the aluminum alloys listed in Table 2.1.1 (EN 1999-1-2), follows from:

$$f_{o,\theta} = k_{o,\theta} \cdot f_o \tag{2.1.1}$$

where

$f_{o,\theta}$ is 0,2 proof strength at elevated temperature

f_o is 0,2 proof strength at room temperature according to EN 1999-1-1.

For intermediate values of aluminium temperature linear interpolation may be used. The modulus of elasticity of all aluminium alloys after two hours thermal exposure to elevated temperature $E_{al,\theta}$ should be obtained from Table 2.1.2 in EN 1999-1-2.

2.1.4.3 Concrete

For heating rates between 2 and 50 K/min, the strength and deformation properties of compressive concrete at elevated temperatures should be obtained from the stress-strain relationship given in Figure 2.1.7. The stress-strain relationships given in Figure 2.1.7 are defined by two parameters:

the compressive strength $f_{c,\theta}$;

the strain $\varepsilon_{c1,\theta}$ corresponding to $f_{c,\theta}$

Table 3.1 in EN 1992-1-2 gives for elevated concrete temperatures θ_c, the reduction factor $k_{c,\theta}$ to be applied to f_c in order to determine $f_{c,\theta}$ and the strain $\varepsilon_{c1,\theta}$. For intermediate values of the temperature, linear interpolation may be used. The parameters specified in Table 3.1 may be used for normal weight concrete with siliceous or calcareous (containing at least 80% calcareous aggregate by weight) aggregates. Values for $\varepsilon_{cu1,\theta}$ defining the range of the descending branch may be taken also from Table 3.1, see EN 1992-1-2.

For thermal actions in accordance with EN 1991-1-2 Section 3 (natural fire simulation), particularly when considering the descending temperature branch, the mathematical model for stress-strain relationships of concrete specified in Figure 2.1.7 should be modified.

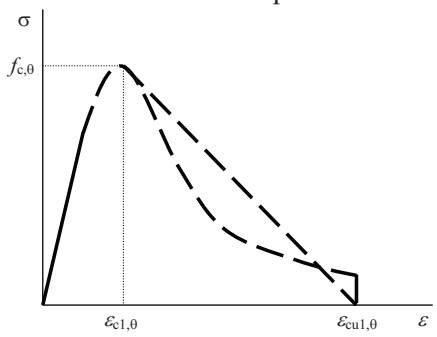

Figure 2.1.7. Mathematical model for stress-strain relationships of concrete under compression at elevated temperatures.

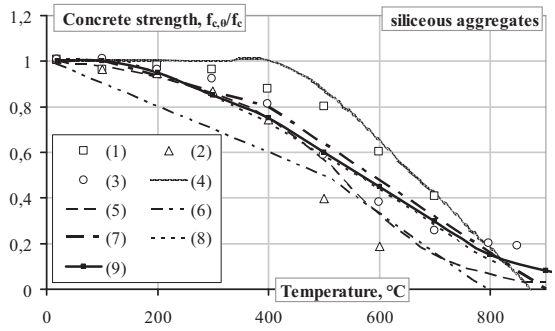

Figure 2.1.8. Comparison of experimental (1−3) and predicted (4−9) strengths of compressive concrete subjected to fire: (1) T. T. Lie, (2) H. L. Malhotra, (3) M. S. Abrams, (4) T. T. Lie and T. D. Lin, (5) K. D. Hertz, (6) T. T. Lie et al, (7) STR 2.05.11:2005 (Lithuanian Code), (8) L. Li ir J. A. Purkiss, (11) EC2.

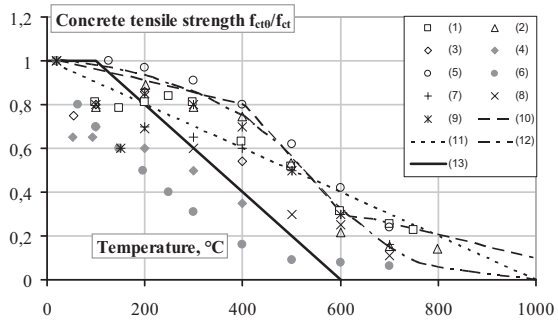

Figure 2.1.9. Comparison of experimental (1−9) and predicted (10-13) strengths of tensile concrete subjected to fire: (1) T. T. Lie, (2) Y. Anderberg and S. Thelandersson, (3), (4) Blundell, (5), (6) Z. P. Bažant and J. C. Chern, (7), (8) Sager, (9) U. Schneider, (10) Z. P. Bažant and J. C. Chern, (11) J. Xiao and G. Konig, (12) M. J. Terro, (13) EC2.

The tensile strength of concrete may be assumed to be zero, which is on safe side. If it is necessary to take account of the tensile strength, when using the simplified or general calculation method may be used. The reduction of the tensile strength of concrete is allowed for by the coefficient $k_{ct,\theta}$ for which $f_{ct,\theta} = k_{ct,\theta} f_{ct}$. In absence of more accurate information $k_{ct,\theta}$ values specified in Figure 2.1.3.2 (EN 1991-1-2) should be used.

The main factors affecting the compressive and tensile strength of concrete are mix proportions, water/cement ratio, aggregate/cement ratio, type of aggregate (Schneider & Horvath 2003). Comparison of experimental and predicted strengths of compressive and tensile strength of concrete subjected to fire is presented in Figure 2.1.8 and 9, respectively.

The strain components at any stress level can be modelled using the superposition theory whereby the total strain is considered to be the sum of various strain components (Schneider & Horvath 2003):

$$\varepsilon_{tot} = \varepsilon_{\sigma}\left(\overline{\sigma}, \sigma, \theta\right) + \varepsilon_{th}\left(\theta\right) + \varepsilon_{tr,cr}\left(\sigma, \theta, t\right) \tag{2.1.2}$$

where ε_{tot} is the total strain, ε_{σ} is the stress–related strain, ε_{th} is the thermal strain, $\varepsilon_{tr,cr}$ is the transient creep strain often called *load induced thermal strain*, θ is the temperature, t is the time, σ is a stress, $\overline{\sigma}$ is the stress history.

The stress–related strain is a function of the applied stress and the temperature. It may be split into elastic and plastic part. The thermal strain is the free thermal expansion resulting from fire temperatures. It is mainly influenced by the type and amount of aggregate. Calculation of thermal strain for concrete is given in the section 4.3 of the technical sheet. The main factor affecting the thermal strain is the type of aggregate. The coarse aggregate fraction plays a dominant role (Schneider & Horvath 2003). Transient creep strain or load induced thermal strain (lits) develops during first heating under load. It is unique to concrete amongst structural materials. Lits is much larger than the elastic strain, and contributes to a significant relaxation and redistribution of thermal stresses in heated concrete structures. Any structural analysis of heated concrete that ignores lits will, therefore, be wholly inappropriate and will yield erroneous results, particularly for columns exposed to fire. This phenomenon is still not fully appreciated by structural engineers and should be incorporated more fully into standards and design codes, Khoury (2000). The main factors affecting the transient strain are type of aggregate, aggregate/cement ratio, curing conditions, loading level (Schneider & Horvath 2003). Mathematical models for transient thermal strain calculations are reviewed by Youssef & Moftah (2007).

It is evident that one could add a shrinkage strain component to Equation 2. However, since all experimental high temperature data are reported from unsealed test conditions the shrinkage component can be viewed as being included in the thermal strain. Furthermore, shrinkage is assumed to be independent of loading (Nielsen et al. 2004).

The other phenomenon of concrete at high temperatures is explosive spalling, which results in loss of material, reduction in section size and exposure of the reinforcing steel to excessive temperatures. Spalling is the violent or non-violent breaking off of layers or pieces of concrete from the surface of a structural element when it is exposed to high and rapidly rising temperatures (Khoury 2000).When the moisture content of the concrete is less than 3% by weight ex-

plosive spalling is unlikely to occur. Above 3% more accurate assessments, moisture content, type of aggregate, permeability of concrete and heating rate should be considered. Spalling can be grouped into four categories: (a) aggregate spalling; (b) explosive spalling; (c) surface spalling; (d) corner/sloughing-off spalling. The first three occur during the first 20–30 min into a fire and are influenced by the heating rate, while the fourth occurs after 30–60 min of fire and is influenced by the maximum temperature. The main parameters affecting the spalling effect are content of moisture in concrete, the heating condition, compressive stresses, thickness of concrete, position of reinforcement, mix proportion, fibre volume (Schneider and Horvath 2003). The prediction of spalling is now becoming possible with the development of thermo-hydro-mechanical nonlinear finite element models capable of predicting pore pressures (Khoury 2000).

2.1.4.4 Stones

Natural stones are considered as less sensitive materials to fire. According to testing of different natural stone types at various temperatures, it has been proved that fire can cause rapid and irreversible physical changes (Hajpál & Török 2004, Hajpál 2008). These alterations negatively influence the strength and static behaviour of the whole monument (Hajpál 2008). Test results have shown that the compressive strength of various lithologies depends on the heating temperature. It can be observed, that the heating does not cause a decrease in the strength for all rock types. The Balatonrendes and Ezüsthegy sandstone and also the Egertihamér rhyolite tuff have higher strength after the heating at 900°C than at room temperature The limestone types lost their strength only at elevated temperatures (Fig. 10).

Strength parameters and axial deformation of limestone do not change uniformly. The tests have demonstrated the differences of compressive stress and axial deformation with increasing temperature (Fig. 11).

Indirect tensile strength of limestone shows slight increase up to 150°C, which is followed by a decrease, while the tensile strength of sandstones and rhyolite tuff do not reflect a clear trend with increasing temperature (Fig. 12).

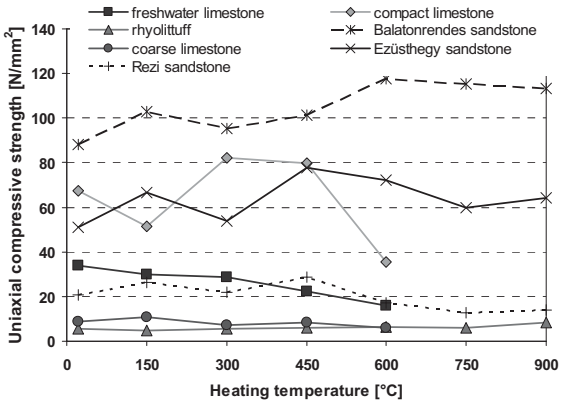

Figure 2.1.10. Uniaxial compressive strength of different stone types as function of the heating temperature.

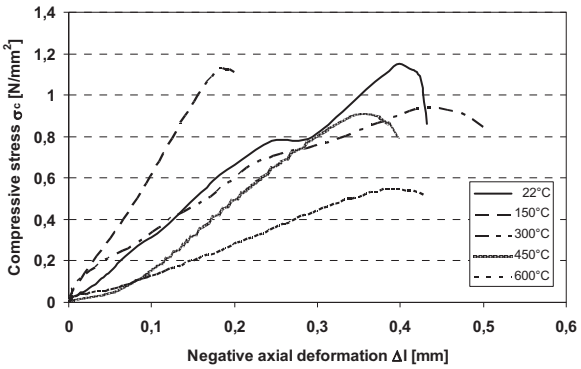

Figure 2.1.11. Compressive stress as function of the negative axial deformation of a coarse limestone at after heating on different temperature.

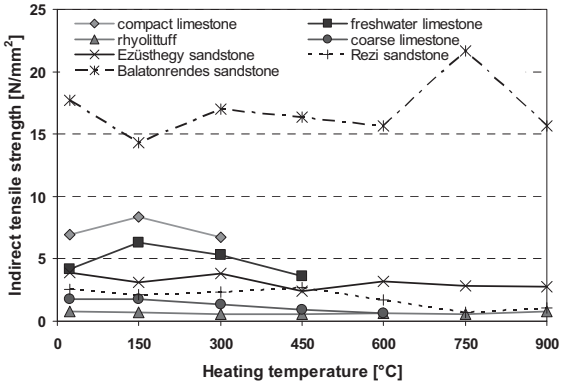

Figure 2.1.12. Indirect tensile strength as function the heating temperature by different stone types.

2.1.5 LOADING, BOUNDARY AND INITIAL CONDITIONS

In engineering practice there are typically two loading and heating scenarios taken into account. One scenario considers increasing static loading in constant elevated temperature. This scenario is used to determine critical loading for selected temperatures. In the second scenario the structure is analyzed under constant mechanical loading but at increasing temperature. The objective for the case of structural steel members is to determine the critical temperature and time. Using repeatable calculations following both scenario diagrams, shown in Figure 2.1.13, load-temperature-time relationships can be formulated and for assumed loading L the fire resistance can be determined in terms of critical temperature T_{cr} or critical time t_{cr}.

In the third scenario, e.g. following experiment or actual fire, both temperature and loading are time depended. Loading can be temperature dependant due to thermal elongation.

Defined mechanical boundary conditions, loading and interactions should be relevant with the actual features of the analyzed member or structure. Depending on the type of analysis, the mechanical loading can be represented by pressures and forces, or prescribed displacements. If necessary, the time or temperature dependent boundary conditions can be represented by contact definitions.

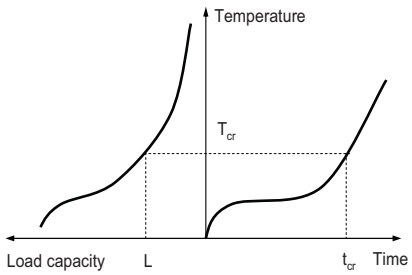

Figure 2.1.13. Determination of fire resistance for assumed loading, Kosiorek (2002).

2.1.6. THERMAL CONDITIONS

Depending on the considered loading scenario, thermal conditions can be modelled applying variety of time and temperature dependent boundary conditions including prescribed temperature fields, insulation, flux, convection, and radiation.

Direct thermal loading. Prescribed temperatures as functions of time are applied to the model nodes (including internal). Relevant for structural analysis without heat conduction.

Constant or time dependent prescribed temperatures applied to selected nodes, on external model surfaces. In this simplified approach heat transfer between surroundings and the model external surfaces is not analysed. Heat transfer inside the model is included, which is applicable for insulation layers.

For the full insulation is the heat transfer on the model surface fully inhibited.

Prescribed flux, applied to external model surfaces. The flux can be time or temperature dependent or constant through analysis and can be used for thermal or coupled structural-thermal analysis. This option requires reliable data specifying the flux magnitude.

Heat transfer between a member and surroundings, defined in terms of convection and radiation. Convection and radiation can be defined for selected model external surfaces. Applicable for thermal and coupled structural-thermal analysis. Transient convection can be expressed by the following formula (Shapiro 2005) and (EN 1991-1-2, 2002)

$$\dot{h}_{net,c} = \alpha_c \left[T_S(t) - T_M(t) \right] \tag{2.1.3}$$

where: $\dot{h}_{net,c}$ - is net convective heat flux in [W/m^2]

α_c – convective heat transfer coefficient [W/m^{2}K], can be constant or temperature dependent. Depends on the model's material, surface finish, fire protection and type of the surrounding gas (EN1991-1-2, 2002).

T_M – calculated current temperature on the model surface [K],

T_S – prescribed temperature of the surroundings can be constant or time dependent (e.g. nominal temperature curve) [K].

Radiative transfer between gas and member can be expressed as (Shapiro 2005), (EN1991-1-2, 2002):

$$\dot{h}_{net,r} = \varepsilon_m \sigma_{SB} \left[T_S^4(t) - T_M^4(t) \right] \tag{2.1.4}$$

where $\dot{h}_{net,r}$ - is net radiative heat flux in [W/m^2]

ε_m – surface absorptivity (emissivity) coefficient can be constant or time/temperature dependent (Hallquist 2006). Depends on the model's material, surface finish, and fire protection,

σ_{SB} – is the Stefan Boltzmann constant [5,67 × 10^{-8} W/m^{2}K^4],

T_M and T_S - the same as above [K].

Compound convective heat transfer can also be used with resultant heat transfer coefficient including radiation effects (EN1991-1-2, 2002).

2.1.7 *BEHAVIOUR AND MODELLING ASPECTS*

2.1.7.1 Stability check for unbraced steel rigid frames in case of fire

At normal temperature design, where it is necessary to consider the influence of the deformed geometry of the structure (2nd order effects) to verify the stability of columns belonging to a structural framed system, when global frame imperfections are considered but member imperfections are not taken into account, two procedures can be adopted, see EN 1993-1-1, 2005: i) to perform a 2nd order analysis including the effects of lateral displacements and check of the member instability with non-sway buckling lengths; and ii) to perform a 1st order analysis and check of the member instability with sway buckling lengths. For the first procedure, it should be noted that non-sway effective lengths can be used because no sway will occur in addition to that which causes the second-order effects calculated by a P-Δ second-order analysis. For sake of simplicity, when using the first methodology, the buckling length of a member may be taken as its system length, which is safe and suggested by the EN 1993-1-1, 2005, for normal temperature design. In fire situation, EN 1993-1-2, 2005, states that, using simple calculation methods, a global analysis of the frame should be done as for normal temperature and the "buckling length l_{fi} of a column for the fire design should generally be determined as for normal temperature design". However, in the case of a braced frame in which each storey comprises a separate fire compartment with sufficient fire resistance, the buckling length, l_{fi}, of a continuous column may be taken as 0,5L in an intermediate storey and 0,7L in the top storey, where L is the system length in the relevant storey. For unbraced structures no specific guidance is given by the Eurocode. For these cases this work shows that considering a buckling length of the columns in a sway mode, independently of the 2nd order effects being negligible or not (so-called P-Δ effects) at normal temperature, leads to good results, for the case of regular multi-storey buildings. Only few studies were made on that subject. Publication no. 159 from Steel Construction Institute (SCI 1996) proposes for the case of columns in sway frames in fire conditions that the effective slenderness ratio may conservatively be taken as $\bar{\lambda}_\theta = 1.25\bar{\lambda}$ (considering the buckling length equal to the system length). A publication from ECCS (1983) suggests that if a global analysis of the frame is not performed to take account of instability effects at elevated temperature, default critical temperature of 300 ºC should be considered, which is too conservative. A buckling length equal to the system length is also suggested by Wang (1997). A global analysis including the instability effects at elevated temperature is rather complex to be used with simple calculation models, therefore simple and safe procedures should be available for design purpose.

The methodology for fire design with simple calculation models consists on evaluating the internal forces in the structure as for normal temperature considering the accidental load combination for fire situation and then checking the fire resistance of each member separately. This was the procedure adopted in the parametric study carried out in this work where the simple calculation model was performed throughout the software Elefir EN (Vila Real & Franssen 2010) and the advanced calculation model SAFIR (Franssen 2005) was used for comparison.

Part 1.2 of EN 1993-1-2 states that the buckling length l_{fi} of a column for the fire design situation should be determined as for normal temperature design. It is not clear if it should be used the same procedure but considering the mechanical properties of steel, namely the Young's modulus, at elevated temperature. If elevated temperature should be used, the process is not an easy task for design purposes. Due to this difficulty, the Wood method (ECCS 2006) at normal temperature has been used in this work to evaluate the buckling length ratio (l_{cr}/L) of the columns. The buckling lengths at elevated temperature were considered with the same value as at normal temperature, i.e., $l_{fi} = l_{cr}$. According to the Wood method the buckling length of a column in a non-sway or sway mode may be obtained from Figure 2.1.14 and Figure 2.1.15 respectively, function of the distribution factors η_1 and η_2, which are given by:

$$\eta_1 = \frac{K_c + K_1}{K_c + K_1 + K_{11} + K_{12}};\ \eta_2 = \frac{K_c + K_2}{K_c + K_2 + K_{21} + K_{22}} \tag{2.1.5}$$

where K_c, K_1 and K_2 are the flexural stiffness coefficients (EI/L) for the adjacent length of columns, and K_{ij} are the effective beam flexural stiffness coefficient. For beams with double curvature K_{ij} = 1.5 EI/L and for the case of single curvature K_{ij} = 0.5EI/L.

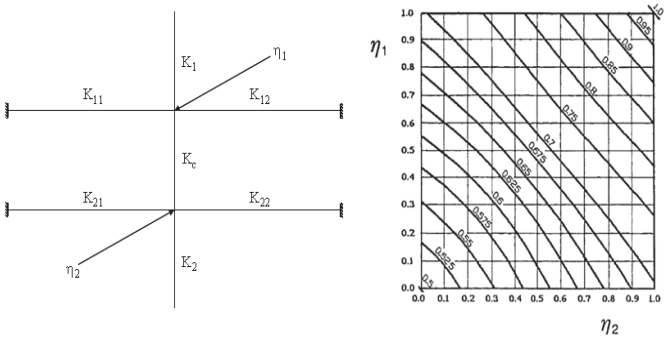

Figure 2.1.14. Buckling coefficient l_{cr}/L for non-sway frames.

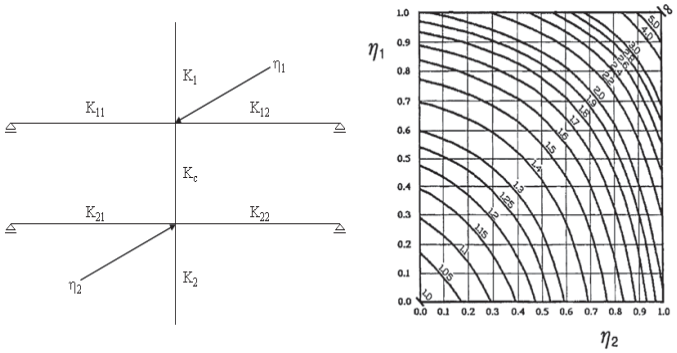

Figure 2.1.15. Buckling coefficient l_{cr}/L sway frames.

In this work for checking the fire resistance of unbraced steel frames by simple calculation models, the internal forces were obtained at normal temperature performing a first order analysis and the member instability was checked using sway buckling lengths. Buckling lengths equal to the system length were also used for comparison.

Beams were assumed to be heated on three sides and all the columns on four sides by the nominal standard fire curve.

Starting from an unbraced steel frame of a three bay – three storey office building shown in Figure 2.1.16, several combinations of different numbers of bays and storeys were considered in the parametric study. This frame has been analysed at normal temperature in the publication no. 119 from ECCS (2006). The members are made of hot-rolled profiles of steel grade S235 being the external columns in HE 220 B, the internal columns in HE 260 B, the intermediate beams in IPE 450 and the top beams in IPE 360.

The structure was assumed to be braced in the out of plane direction and unbraced in the plane of the frame. Out of plane column buckling is prevented and lateral restraint is assumed to be provided to the beams by the concrete floor and roof slabs. The columns are continuous throughout of the full height of the building.

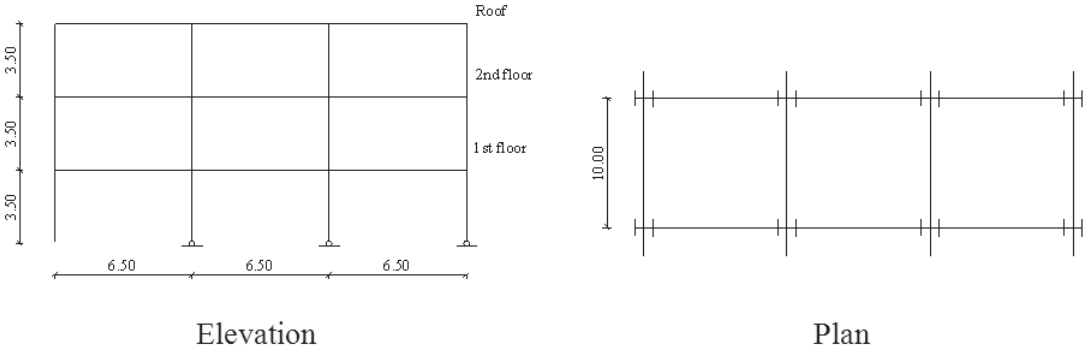

Figure 2.1.16. Frame geometry.

Table 2.1.1. Load combination cases.

Load combination	Accidental Combination
Case 1	$G_k + 0.2W_k$
Case 2	$G_k + 0.5I_1$
Case 3	$G_k + 0.5I_2$
Case 4	$G_k + 0.5I_3$
Case 5	$G_k + 0.2W_k + 0.3I_1$
Case 6	$G_k + 0.2W_k + 0.3I_2$
Case 7	$G_k + 0.2W_k + 0.3I_3$

The load combinations for accidental fire situation used are listed in Table 2.1.1, where G refers to the permanent loading, W to the wind loading and I_1, I_2 and I_3 to the imposed loads alternation.

Frame imperfections due to unavoidable initial out-of-plumb were taken into account prescribing a notional horizontal force that was applied at each story level, see EN 1993-1-1, 2005.

A parametric study has been performed considering several combinations of bays and storeys from 1x1 to 3x3 in a total of 9 unbraced frames as shown in Figure 2.1.17. The frames were considered to be pinned or fixed at the supports and the seven load combinations presented in Table 2.1.1 were considered.

The fire scenarios used with the advanced calculation model were the standard fire acting in each storey separately from the ground floor to the upper floor.

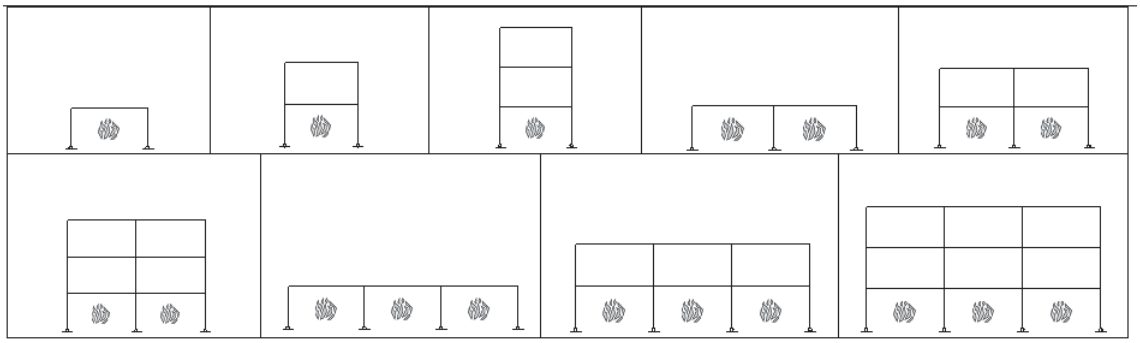

Figure 2.1.17. Frame geometry used in the parametric study.

The results of the parametric study plotted in Figure 2.1.18 show that the proposal made to consider the sway buckling lengths in the case of unbraced frames is mostly on the safe side when compared with the advanced calculation method. This Figure 2.1.also shows that if the system length is considered for the buckling length the results are too unsafe.

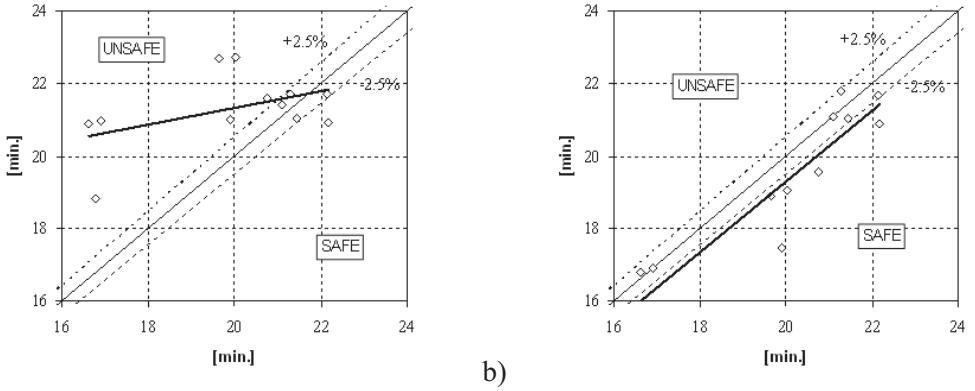

Figure 2.1.18. Comparison between simple calculation model (Elefir-EN) and advanced calculation model (SAFIR). a) $l_{fi} = L$; b) $l_{fi} = kL$ (k obtained with Wood method for-sway frames).

2.1.7.2 Computer simulation of a steel connection at elevated temperature

Experiments and components based models are the most reliable source of information on responses of structural connection at ambient as well as elevated temperature. With the increasing computing capabilities nowadays, it is possible using the Finite Element Method to simulate complex cases and consider wide range of parameters. As an example Figures 2.1.19 - 2.1.22 show results of a feasibility study on a coupled structural thermal analysis of a beam to column connection subjected to fire, Tybura & Kwaśniewski (2008). Numerical results in the form of moment-rotation characteristics are compared with the published data for a selected flush end-plate connection, Al-Jabria et al. (2006). The Finite Element analysis is conducted using commercial program LA-DYNA®, Hallquist (2006). The considered connection consist of two 254 x 102 UB 22 beam segments connected to a 152 x 15 2UC 23 column using 8 mm thick flush end plate and six M16 bolts. The test setup and all dimensions are provided in Al-Jabria et al. (2006).

Several three dimensional simplified FE models were developed using 4 – node shell elements for the purpose of a global analysis intended for a large scale structure. The model, shown in Figure 2.1.19, represents one fourth of the configuration. This model is appropriate for symmetrical loading and temperature conditions. The bolts are represented by 1D beam elements connected to rigid shell elements in end plate and column flange, used to better distribute forces around bolts heads and nuts.

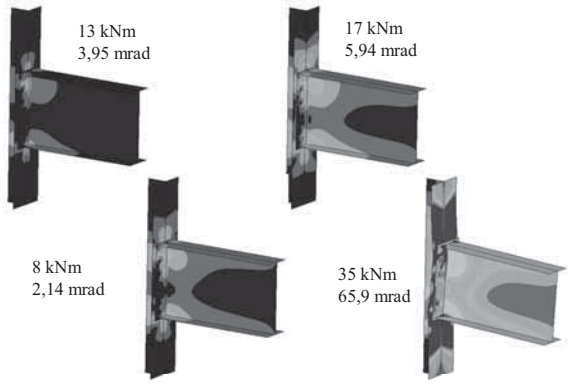

Figure 2.1.19. Contours of Mises stress under increasing mechanical loading at constant ambient temperature 20 °C.

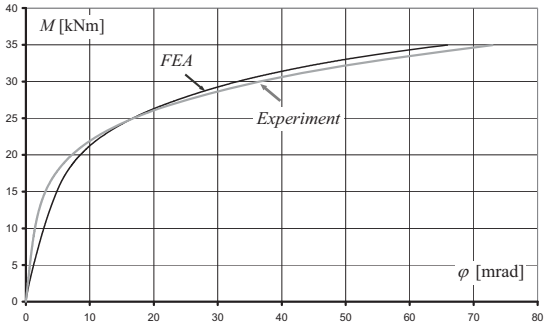

Figure 2.1.20. Moment versus rotation curve at constant temperature 20 °C.

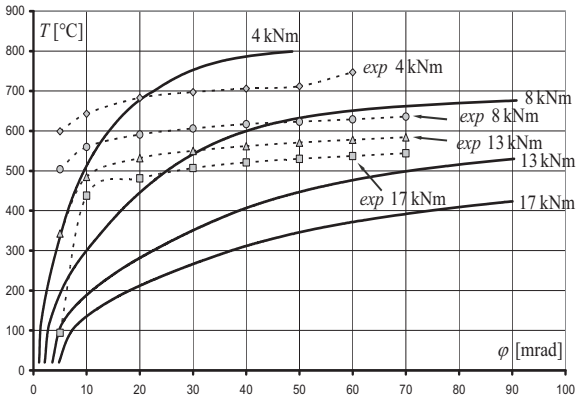

Figure 2.1.21. Temperature versus rotation.

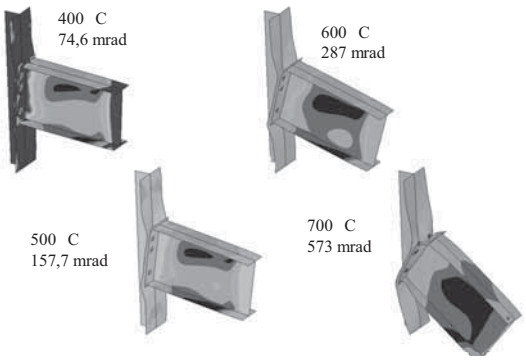

Figure 2.1.22. Contours of Mises stress for bending moment 17 kNm and increasing temperature.

A temperature dependent elastic – plastic material model with strain hardening, was applied. It allows for relating material parameters such as: elastic modulus, Poisson's ratio, coefficients of thermal expansion, yield stress, and plastic hardening modulus to temperature, represented in a discrete way at selected points. All components of the tested connection, except the bolts, were made of steel S275. The stress-strain relationships of the steel S275 at elevated tempera-

tures, calculated based on the EN 1993-1-2, 2005a. For coupled structural thermal and thermal only analyses, thermal properties such as heat capacity and thermal conductivity are specified in the additional material model, called thermal isotropic, Hallquist (2006). All thermal parameters can also be defined as temperature dependent. For the bolts assumed yield and ultimate stresses were 480 and 600 MPa, respectively, Al-Jabria et al. (2006).

Depending on the considered case, the loading can be performed as a predefined displacement or concentrated force applied to a selected node rigidly connected with the beam segment. The top and the bottom the column and the middle section of the column web are constrained. For the model of one forth of the test configuration additional constraints are applied on the vertical symmetry plane. Included in the FE model segments of the beam and the column represent regions with the maximum deformation, where the influence of the assumed boundary conditions can be neglected. In the FE model the beam is connected to the column through contact between column flanges, end plate and bolts. Due to internal complexity of con-tact algorithms incorporated in the FE programs, an analysis including contact is usually challengeable, can affect results and even lead to problems with convergence.

The calculated results were compared with the experimental data presented in the paper, Al-Jabria et al. (2006). All structural analysis presented here are based on static calculation using implicit solver, where instead of physical time a loading parameter is applied, Hallquist (2006). The temperature is applied uniformly to all the nodes, simulating furnace test conditions. Depending on considered case during the simulation temperature is constant or increases with the loading parameter.

In Figure 2.1.20 are compared calculated and experimental relationships between moment and rotation for increasing loading at ambient temperature 20 °C. Figure 2.1.19 presents contours of Mises stress for the same loading case.

Curves in Figure 2.1.21 show calculated relationships between temperature and rotation, for four loadings producing moments at the connection M = 4, 8, 13, and 17 kNm. The loading is applied gradually at the begging of the simulation and then kept constant while the temperature is increased from 100 to 800 °C. Points in Figure 2.1.21 represent experimental values. Comparison with the experiment shows higher resistance of the FE model, mainly due to overestimated material parameters for larger strains. Figure 2.1.22 shows contours of effective Mises for bending moment 17 kNm and increasing temperature. In all figures the Mises effective stress is mapped with the same gray and heat transfer. Chosen material model allows only for coarse piecewise linear approximation of stress – strain relationships through specification of hardening modulus. This approach leads to overestimated stresses for higher strain values and results with higher loading values comparing to the experimental data. Due to high value of thermal conductivity of steel temperature distribution during fire can be assumed as uniform and heat transfer does not have to be considered. For concrete and composite (concrete and steel) structures such approach can be insufficient.

2.1.7.3 Fully coupled temperature-displacement analyses of steel portal frames under fire

The behaviour of steel structures under fire needs particular attention since the structural steel undergoes considerable deterioration in presence of high temperatures, such as the reduction of both resistance and stiffness of steel. This can cause the collapse of structures that are safely designed for ordinary load combinations, in which the fire scenario is disregarded. Consequently, the behaviour in fire of steel structures requires deep investigations from both experimental and numerical points of view.

Recently a numerical study aimed at investigating the behaviour of steel structures under fire based on the use of fully coupled temperature-displacement finite element analyses, carried out by means of the advanced computer program ABAQUS has been presented (Faggiano et al. 2007a). The used method allows to consider at the same time the mechanical and thermal aspects of the problem. The mechanical and thermal problems are faced up in a unique model, in which the actual phases of the modelled phenomenon, say the sequential application to the structure of the design loads and, then, of the fire scenario, are reproduced in a step-by-step analysis. Such approach differs from the usually adopted one, which consists, for the sake of simplicity, in performing the heat transfer analysis and the mechanical one separately (uncoupled analyses): the first one allows to evaluate the temperature-time law within the structural

elements exposed to fire, completely neglecting the stress-displacement aspect; the second one consists in the usual structural analysis, in which the structure is subjected to the external loads; at the end of the structural analysis, the temperature-time variation, obtained from the preliminary heat transfer analysis, is imposed to the structural members, so allowing the calculation of the fire resistance of the structure. On the contrary, in the case of fully coupled temperature-displacement analyses, the used finite elements are endowed with both displacement and temperature degrees of freedom, so that the mechanical and thermal equations are written simultaneously and the mutual interactions between the two aspects of the problem can be easily caught.

The study dealt with simple steel portal frames, focusing on the main geometrical and mechanical parameters that influence the fire resistance of the considered structures, such as the span over height ratio, the passivity ratio of the structural members, the steel grade and the exploitation degree of the material (Faggiano et al. 2007a). However such a methodology was already applied for the investigation of the behaviour of steel structures exposed to fire after being damaged by an earthquake (Faggiano et al. 2007b). Other studies on the subject, based on different approaches, are presented in (Della Corte and Landolfo, 2001; Della Corte et al. 2003a, b; Della Corte et al. 2005; Faggiano et al. 2005).

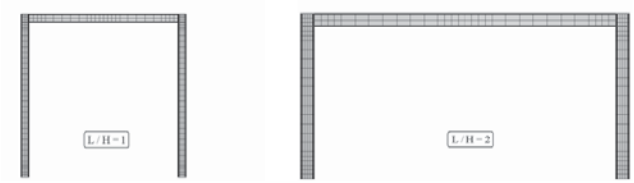

Figure 2.1.23. Finite element meshes of the models (Faggiano et al. 2007a).

2.1.7.4 Simplified tool for analysis of RC members under fire

Lack of experimental and theoretical investigations on behaviour of RC members under high temperatures hampers development of the constitutive laws. Compressive strength does serve as a sufficient parameter to characterize thermal, physical and mechanical properties of concrete at elevated temperatures. Geda (2010) performed a comprehensive study aiming at numerical analysis of thermo-mechanically loaded RC members. The analysis has shown that:

1) A universal thermal and physical-mechanical model for concrete has not been proposed until now. Due to limited experimental and theoretical investigation of behaviour of RC members, the material models are not accurate.

2) Compressive strength of concrete is not a sufficient parameter characterizing thermal, physical and mechanical properties of concrete at elevated temperatures.

3) Most physical and thermo-mechanical parameters are most accurately characterized by the EN 1992-1-2, 2004.

4) Some characteristics of concrete were best predicted by other models: modulus of elasticity by Xiao & Konig (2004), strain corresponding to maximal stress by Khennane & Baker (1993), limit strain by Terro (1998), transient creep strain by Anderberg & Thelandersson (1976).

The behavior of RC structures at elevated temperatures is very complex. With rising temperature, thermal, physical and mechanical properties of concrete and reinforcement significantly change. Analytical and computation methods (Huang et al. 1999, Bratina et al. 2007, Capua Di & Mari 2007, and Kodur & Dwaikat 2008) have been extensively developed in the field of RC building exposed to high temperature or accidental fire. However, in the analysis an engineer usually employs various formulae for the fire resistance of structures offered by building codes (CEN 2004), without really understanding the thermo-mechanical behavior of a structure during fire (Bratina et al. 2007). On the other hand, advanced non-linear mechanical models based on the 2D or 3D finite element (FE) method (Huang et al. 1999, Cervenka et al. 2005, and Capua Di & Mari 2007) which were rapidly progressing within last three decades are based on universal principles and can include all possible effects. However, such methods are highly demanding

in terms of the computational recourses. Besides, the constitutive laws taking into account the high temperature effects are not accurate enough. Recent fires with fatalities stimulate new investigation wave for providing fire resistance in reinforced concrete structures subjected to high temperature. Analytical and numerical methods are widely used for analysis of fire resistance in reinforced concrete structures. However, advanced FE methods based on non-linear material models are highly expensive in terms of the computational time. Therefore, their application is limited to simple cases.

A numerical procedure, based on *Layer* section model and smeared crack approach, aiming at deformation analysis of bending RC members, has been developed and improved at Vilnius Gediminas Technical University. The procedure assures higher accuracy of deflection predictions in comparison to the design code methods. An efficient combination of accuracy and simplicity has been achieved in the Layer section model. This allowed incorporating it into a simple engineering technique based on classical principles of strength of materials extended to layered approach and use of full material diagrams.

In this study, an attempt has been made to extend application of the Layer section model to stress and strain analysis of RC bending members subjected to high temperature, taking into account non-linear physical and thermo-mechanical materials properties. Proposed numerical procedure is developed to assess the stress-strain state, load bearing capacity and failure time of RC members. This approach is very effective in terms of computer resources, i.e. the calculation time decreases hundreds of time in comparison to standard non-linear FE programs (MSC.MARC, DIANA, and ATENA).

The Layer section model for RC members subjected to elevated temperatures is based on the following assumption and approaches:

1) Smeared crack approach, i.e. average stresses and strains are used.

2) Linear distribution of strain within the depth of the section, i.e. the *Bernoulli* hypothesis is adopted.

3) Perfect bond between concrete and reinforcement is assumed; reinforcement slippage occurring at advanced stress-strain states is included into stress-strain diagram of tensile concrete.

4) Temperature is increasing, i.e. the cooling-down stage is not considered.

5) Thermal strain as well as transient creep strain are assessed as equivalent axial forces and bending moments.

Behaviour of compressive concrete and reinforcement is modelled according to EN 1992-1-2, 2004. Behaviour of tensile concrete is modelled by the bilinear stress-strain relationship shown in Figure 2.1.24 with tensile strength and modulus of elasticity taken from EN 1992-1-2, 2004In this figure, θ is the temperature arising in the layer. The descending branch of the diagram is characterized by the ultimate strain ε_{ctu} (Kaklauskas 2004):

$$\varepsilon_{ctu} = \left(32.8 - 27.6p + 7.12p^2\right)\frac{f_{ct}}{E_c} \tag{2.1.6}$$

Here p is the tensile reinforcement ratio (%); f_{ct} and E_c are the tensile strength and the modulus of elasticity of concrete, respectively. The latter two parameters are derived according to EN 1992-1-2, 2004.

A cross-section as shown in Figures 2.1.25a and 2.1.25b is divided into a number of layers corresponding to either concrete or reinforcement. Temperature gradient, Figure 2.1.25c, within the section was determined in the using the approaches and assumptions of heat transfer theory. Nonlinear distribution of high temperatures was replaced by equivalent axial force and bending moment.

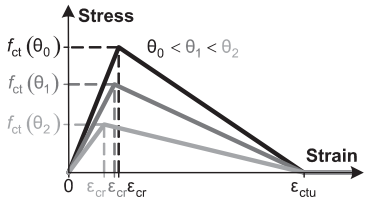

Figure 2.1.24. Constitutive law for cracked tensile concrete.

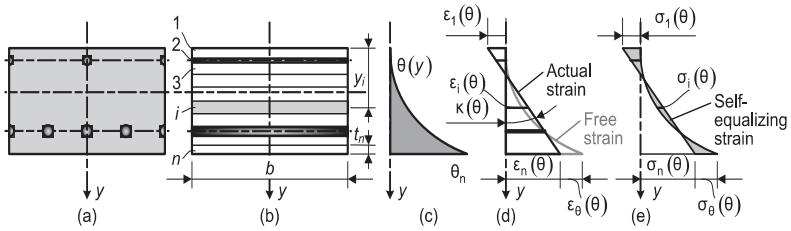

Figure 2.1.25. Stress and strain caused by non-linear temperature gradient (Bacinskas et al. 2008): RC cross-section (a); Layer section model (b); temperature gradient (c); distribution of strain (d) and stress across the section (e).

Variable mechanical and physical properties of every layer can be evaluated in the analysis duo to loading and temperature effect. Cross-section of RC members is replaced by transformed concrete sections. This is performed by multiplying area of *i*-th layer by ratio of modulus of elasticity $E_{\mathrm{i}}'\left(\theta,\varepsilon_\sigma\right)/E_{\mathrm{c}}\left(20\,^{\circ}\mathrm{C}\right)$, where $E_{\mathrm{i}}'\left(\theta,\varepsilon_\sigma\right)$ is the temperature-dependent secant modulus of elasticity of *i*-th layer, $E_{\mathrm{c}}\left(20\,^{\circ}\mathrm{C}\right)$ is the modulus of elasticity of concrete at normal temperature. Geometrical characteristics of transformed cross-section (area $A_{\mathrm{c,eff}}$, first moment $S_{\mathrm{c,eff}}$ and second moment of inertia $I_{\mathrm{c,eff}}$) determined about the top edge of the section:

$$A_{\mathrm{c,\,eff}}=\sum_{\mathrm{i}=1}^{\mathrm{n}}b_{\mathrm{i}}t_{\mathrm{i}}E_{\mathrm{i}},\quad S_{\mathrm{c,\,eff}}=\sum_{\mathrm{i}=1}^{\mathrm{n}}b_{\mathrm{i}}t_{\mathrm{i}}y_{\mathrm{i}}E_{\mathrm{i}},\quad I_{\mathrm{c,\,eff}}=\sum_{i=1}^{n}\left(\frac{b_{\mathrm{i}}t_{\mathrm{i}}^3}{12}+b_{\mathrm{i}}t_{\mathrm{i}}y_{\mathrm{i}}^2\right)E_{\mathrm{i}},\quad E_{\mathrm{i}}=\frac{E_{\mathrm{i}}'\left(\theta,\varepsilon_\sigma\right)}{E_{\mathrm{c}}\left(20\,^{\circ}\mathrm{C}\right)}. \tag{2.1.7}$$

Here *n* is the total number of layer; b_{i} and t_{i} are the width and the thickness of the *i*-th layer, respectively; y_{i} is the distance of *i*-th layer from the top of the section.

Concrete total strain can be expressed as follows:

$$\varepsilon_{\mathrm{tot}}\left(\theta,\sigma\right)=\varepsilon_\sigma\left(\theta,\sigma\right)+\varepsilon_{\mathrm{th}}\left(\theta,\theta_0\right)+\varepsilon_{\mathrm{ttc}}\left(\theta,\sigma\right). \tag{2.1.8}$$

Here $\varepsilon_\sigma\left(T,\sigma\right)$ is the stress-induced strain; $\varepsilon_{\mathrm{th}}\left(\theta,\theta_0\right)$ is the thermal strain; and $\varepsilon_{\mathrm{ttc}}\left(\theta,\sigma\right)$ is the strain due to transient thermal creep.

Thermal-induced strain in the *i*-th layer can be expressed as follows:

$$\varepsilon_{\mathrm{th,i}}\left(\theta,\theta_0\right)=\alpha_{\mathrm{i}}\cdot\Delta\theta_{\mathrm{i}};\quad \Delta\theta_{\mathrm{i}}=\theta_{\mathrm{i}}-\theta_0. \tag{2.1.9}$$

Here α_{i} is the coefficient of thermal expansion of *i*-th layer. It is recommended to calculate this coefficient according to EN-1992-1-2, 2004, recommendation.

Transient thermal creep strain for tensile concrete layers is neglected. The strain for compressive concrete can be calculated according to Anderberg & Thelandersson (1976):

$$\varepsilon_{\mathrm{ttc,i}}\left(\theta,\sigma\right)=\varepsilon_{\mathrm{th,i}}\left(\theta,\theta_0\right)\frac{\beta\cdot\sigma_{\mathrm{i}}}{f_{\mathrm{c}}\left(20\,^{\circ}\mathrm{C}\right)}. \tag{2.1.10}$$

Here β is the material coefficient, which varies from 1.8 up to 2.35; σ_{i} is the compressive stress in the *i*-th layer; $f_{\mathrm{c}}\left(20\,^{\circ}\mathrm{C}\right)$ is the compressive strength of concrete under normal condition. Transient thermal creep strain is taken negative.

It should be noted that temperature in the cross-section of the element under fire is distributed non-uniformly. Furthermore, physical and mechanical properties of layers are varying. Free extension of every layer is limited by adjacent layers. Therefore, bending stresses, see Figure 2.1.25e, arise in the element cross-section due to layer mutual interaction.

Influence of strains $\varepsilon_{\mathrm{th}}\left(\theta,\theta_0\right)$ and $\varepsilon_{\mathrm{ttc}}\left(\theta,\sigma\right)$ on the stress-strain state of RC member can be evaluated by introducing equivalent axial forces and bending moments. Equivalent axial force can be defined as a sum of appropriate stresses:

$$N_{\mathrm{th}}=\sum_{\mathrm{i}=1}^{\mathrm{n}}\sigma_{\mathrm{th,i}}b_{\mathrm{i}}t_{\mathrm{i}}=\sum_{\mathrm{i}=1}^{\mathrm{n}}\varepsilon_{\mathrm{th,i}}\left(\theta,\theta_0\right)E_{\mathrm{i}}'\left(\theta,\varepsilon_\sigma\right)b_{\mathrm{i}}t_{\mathrm{i}};\quad N_{\mathrm{ttc}}=\sum_{\mathrm{i}=1}^{\mathrm{n}}\sigma_{\mathrm{ttc,i}}b_{\mathrm{i}}t_{\mathrm{i}}=\sum_{\mathrm{i}=1}^{\mathrm{n}}\varepsilon_{\mathrm{ttc,i}}\left(\theta,\theta_0\right)E_{\mathrm{i}}'\left(\theta,\varepsilon_\sigma\right)b_{\mathrm{i}}t_{\mathrm{i}}. \tag{2.1.11}$$

Equivalent bending moments can be determined analogically:

$$M_{\text{th}} = \sum_{\text{i=1}}^{\text{n}} \varepsilon_{\text{th,i}}\left(\theta,\theta_0\right) E_{\text{i}}'\left(\theta,\varepsilon_\sigma\right) b_{\text{i}} t_{\text{i}} y_{\text{i}}; \quad M_{\text{ttc}} = \sum_{\text{i=1}}^{\text{n}} \varepsilon_{\text{ttc,i}}\left(\theta,\theta_0\right) E_{\text{i}}'\left(\theta,\varepsilon_\sigma\right) b_{\text{i}} t_{\text{i}} y_{\text{i}}. \quad (2.1.12)$$

Given equivalent actions are applied additionally to the RC element subjected to external loads N_{ext} and M_{ext}:

$$N_{\text{tot}} = N_{\text{ext}} + N_{\text{th}} + N_{\text{ttc}}; \quad M_{\text{tot}} = M_{\text{ext}} + M_{\text{th}} + M_{\text{ttc}}. \quad (2.1.13)$$

Then strain at top fiber and curvature for the section under consideration can be determined:

$$\varepsilon_{\text{tot,l}}\left(\theta\right) = -\frac{I_{\text{c, eff}} N_{\text{tot}} + S_{\text{c, eff}} M_{\text{tot}}}{E_{\text{c}}\left(20\,^{\circ}\text{C}\right)\left(A_{\text{c, eff}} I_{\text{c, eff}} - S_{\text{c, eff}}^2\right)}; \quad \kappa\left(\theta\right) = \frac{S_{\text{c, eff}} N_{\text{tot}} + A_{\text{c, eff}} M_{\text{tot}}}{E_{\text{c}}\left(20\,^{\circ}\text{C}\right)\left(A_{\text{c, eff}} I_{\text{c, eff}} - S_{\text{c, eff}}^2\right)}. \quad (2.1.14)$$

Total strain at any point of the section is defined in terms of above parameters:

$$\varepsilon_{\text{tot,i}}\left(\theta\right) = \varepsilon_{\text{tot,l}}\left(\theta\right) + y_{\text{i}} \cdot \kappa\left(\theta\right). \quad (2.1.15)$$

From expression (3), stress-induced strain in *i*-th layer can be determined as follows:

$$\varepsilon_{\sigma,\text{i}}\left(\theta,\sigma\right) = \varepsilon_{\text{tot,i}}\left(\theta,\sigma\right) - \varepsilon_{\text{th,i}}\left(\theta,\theta_0\right) - \varepsilon_{\text{ttc,i}}\left(\theta,\sigma\right). \quad (2.1.16)$$

Then stress in *i*-th layer is derived using the following equation:

$$\sigma_{\text{i}}\left(\theta\right) = \varepsilon_{\sigma,\text{i}}\left(\theta,\sigma\right) \cdot E_{\text{i}}'\left(\theta,\varepsilon_\sigma\right). \quad (2.1.17)$$

In Equation 2.1.16, transient creep strains for layers, which correspond to reinforcement and tensile concrete, are assumed to be equal to zero.

Proposed numerical procedure for deformational analysis of RC members subjected to thermo-mechanical loading has been performed iteratively by the following steps:

1. Geometrical characteristics are calculated for the transformed cross-section by Equation 2.1.7. In the first iteration, linear materials properties are assumed both for concrete and steel layers taking into account temperature effects.

2. Equivalent axial forces and bending moments are calculated by Equations 2.1.11 and 2.1.12. Total actions applied to the element are obtained using Equation 2.1.13. In the first iteration, transient thermal creep-induced actions are assumed to be equal to zero.

3. Strain at top fibre and curvature are calculated using Equation 2.1.14.

4. Total strain is derived by Equation 2.1.15 for each of layers.

5. For the assumed constitutive law of reinforcement and concrete, stress is calculated using Equation 2.1.12 for each of layers. Secant deformational modulus in the layer is determined as a ratio between given stress and stress-induced strain, obtained by Equation 2.1.16.

6. Obtained deformational modulus is compared with previously assumed or calculated one for each of the layers. If the agreement is not within the assumed errors limits, a new iteration is started from step 2. Over vice, obtained values of strains, stresses and curvatures are assessed. For deflection calculation which is performed by Mohr's integral technique, analogous computations are carried out for other sections of the member.

Proposed model can assess the stress-strain state, load carrying capacity and failure time of RC members. This model is simple and versatile. Its simplicity is due to use of classical formulas of mechanics of materials. Application of a uniform model in the short- and long-term analysis (including shrinkage and creep) for both ordinal and pre-stressed RC members under normal and high temperatures characterizes the versatility of the model. The proposed algorithm is very effective in terms of computer resources, i.e. the calculation time decreases hundreds of times (from hours to few seconds) in comparison to standard non-linear finite element programs.

The *Layer* section model has been applied to perform stress and strain analysis of flexural RC members subjected to high temperature, taking into account non-linear physical and thermo-mechanical material properties. A number of numerical studies performed by the authors (see for instance: Gribniak *et al*. 2006, Kaklauskas *et al*. 2007, Bacinskas *et al*. 2008, and Geda 2010) show satisfactory accuracy and computational effectiveness of the proposed procedure. To illustrate application of the procedure, a comparison between the computed, using the described procedure, and the measured RC slab deflections is presented in the next section.

This section presents a comparison between the predicted and measured RC slab deflections reported by Cook (2001). It includes results of modelling of two floor slabs (namely Slab 1 and Slab 2) exposed to heating conditions specified by nominal standard fire curve. The specimens were 4700 mm long, 150 mm high and 925 mm wide. The reinforcement cover is 25 mm. The slabs were cast of concrete mixes with siliceous aggregated and designed to have characteristic cube strength of 30 MPa. The reinforcing steel bars were of high yield ribbed bar having yield strength of 460 MPa. Slabs were reinforced with 10 bars of 8 mm diameter. As shown in Figure 2.1.26a, Slab 1 was subjected to high temperature without mechanical loading and Slab 2, shown in Figure 2.1.26b, was also subjected external loading (distributed load q = 1.5 kN/m2).

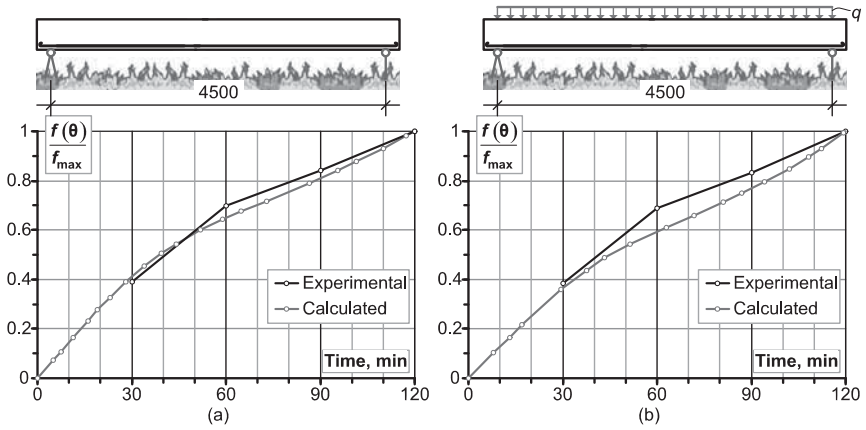

Figure 2.1.26. Normalized deflections of Slabs 1 (a) and 2 (b) subjected to ISO 834 fire conditions.

The temperature distributions within cross-section of both slabs after 30, 60, 90 and 120 min fire exposure were presented in (Cook 2001). These temperature profiles were used for the respective time-deflection analysis of slabs. As temperature dependent material properties were not given in the reference, they were assumed according to EN 1992-1-2-1-2, 2004.

The modelled time-deflection diagrams are presented in Figure 2.1.26 along with the experimental curves. The time-deflections diagrams are presented in terms of normalized deflections, where *f* is the deflection of slab after 120 min of fire exposure.

It can be seen from Figure 2.1.26 that the shape of the experimental load-deflection diagrams was well captured in the present analysis. Agreement of the calculated and measured deflections is within reasonable limits. In both analyses, the deflections were underestimated, but the maximal error has not exceeded 35 %.

In this study, an attempt has been made to extend application of the *Layer* section model to stress and strain analysis of flexural RC members subjected to high temperature. A powerful calculation technique has been developed. Variation of material properties within the section due to different loading and temperature gradient was assessed in the analysis. Restrained thermal deformations as well as transient thermal creep were modelled by means of fictitious equivalent forces. The proposed algorithm is very effective in terms of computer resources, i.e. the calculation time decreases hundreds of times (from hours to few seconds) in comparison to standard non-linear finite element programs. Comparison of the experimental and modelling results has shown that the proposed model has satisfactorily captured the load-deflection behaviour of the precast concrete slabs.

2.1.7.5. Aluminium alloys structures

The prediction of the mechanical response of aluminium alloy structures exposed to fire is complicated for two principal reasons: 1) the difficulty of developing accurate structural analyses in post-elastic field, taking correctly into account the mechanical features of the basic material, such as the strain-hardening and the limited deformation capacity; 2) the inadequate knowledge of the material behaviour under high temperatures. As a consequence, first of all the specific mechanical properties and the whole stress-strain curve of the material as a function of temperature have to be accurately defined. Moreover, the methods of structural analysis in fire conditions should hold in due account the influence of the shape of the material constitutive law and

thus of the kinematic strain hardening on the global behaviour of the structure. Therefore, for allowing practical analysis of complex structures in fire conditions through advanced methods, such accurate material models should be implemented in finite element programs. In this context, a wide examination of the results of experimental tests (ASM Specialty Book, 1993) carried out on different aluminium alloys exposed to high temperatures has been presented (Faggiano et al., 2004a), aiming at characterizing the behaviour under fire in relation to the series and treatments (work hardening state (H), hardening state due to heat treatment (T), annealed state (O)) of the aluminium alloys. The variation laws of the following characteristic parameters has been drawn: the elastic modulus (E), the elastic limit stress conventionally defined as 0.2% proof strength ($f_{0,2}$), the ultimate strength (f_t) and the ultimate deformation (et). Then, a mechanical model, which appropriately represents the peculiarity of such materials subjected to high temperatures, has been proposed, based on the well known Ramberg - Osgood law. The obtained simplified constitutive law has been introduced in a finite element program for the calculus under fire of structures (Franssen, 1998), with specific reference to the aluminium alloys selected for structural uses by the EN 1999-1-2, 2003.

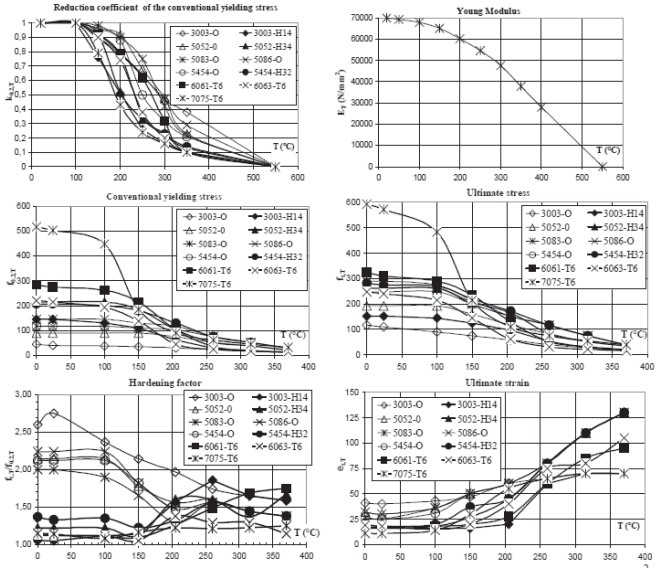

Figure 2.1.27. EC9 aluminium alloy's mechanical properties as function of temperatures (f [N/mm2], et [%]) (Faggiano et al. 2005).

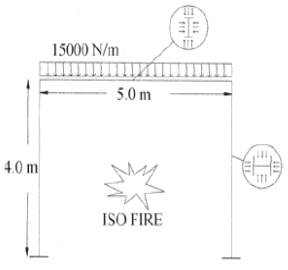

Figure 4. Study cases

ALLOY	$f_{0.2,d}$ (N/mm^2)	Column HEB	Beam IPE
3003-O	45	160	450
3003-H14	145	160	300
5052-O	90	160	330
5052-H34	215	160	240
5454-O	117	160	300
5454-H32	207	160	240
5083-O	145	160	300
5086-O	117	160	300
6061-T6	283	160	240
6063-T6	220	160	240
7075-T6	517	160	240

Figure 2.1.28. Study cases (Faggiano et al. 2005).

Finally, the results of the structural analyses in fire conditions obtained for a simple portal frame and carried out for all the EN 1999-1-2 aluminium alloys have been presented, clarifying the impact of the material modelling on the global response of the structure exposed to fire, evaluated in terms of time up to collapse for a conventional fire scenario, see Faggiano et al., 2003; 2004a,b, 2005.

As a first result of the study, it has been pointed out that simplified mechanical models, such as the elastic-perfectly plastic one, generally are not able to correctly characterize the material

behaviour at the high temperatures, since they disregard the beneficial effect due to continuous material hardening, which is somewhat effective in balancing strength decay due to high temperatures. Therefore, in order to take specifically into account the effect of the strain hardening, the more comprehensive mechanical model for the aluminium alloys proposed is able to represent in an appropriate manner all the peculiarities of such materials exposed to high temperatures. The structural analysis in fire conditions of a study case related to a simple portal frame has pointed out the remarkable effect of material modelling of aluminium alloys, since the adoption of elastic-perfectly plastic model results very conservative and not convenient for a material which exhibits a so rapid strength decay with high temperature. Finally, not treated alloys (O) give rise to the best behaviour under fire due to the beneficial effect of material strain hardening and to the fact that the strength degradation at high temperature is softer than for treated alloys.

2.1.7.6 Composite steel-concrete frames

The advanced calculation models allow to evaluate the structural fire behaviour of single members, substructures and entire structures, see EN 1994-1-2. The topic of this contribution is the application of advanced calculation models for structural fire analysis of composite steel and concrete frames in order to compare the results of member, substructure and global analyses in terms of fire safety assessment (Nigro et al. 2008, 2009). The influence of some aspects of structural response developing during the fire exposure, generally neglected in the member analysis, on the assessment of the structural fire safety is pointed out, such as: indirect fire actions, large displacements, geometric and mechanical non-linearities.

Two composite steel-concrete frames, with four storeys and three spans, are designed for two different seismic zones according to the recent Italian Technical Code (2008). The beams are composite comprising steel beam with no concrete encasement and the columns are partially encased. Each frame has different over-strength of the columns with respect to the beam, due to the capacity design rules and damage limit state requirements of the seismic design. Moreover, in order to improve the fire resistance, composite steel beams with partial concrete encasement are also adopted for both frames. More details of the frame cross-sections are reported in Figure 2.1.29.

Each frame is subjected to different fire scenarios with the nominal standard time-temperature curve, see EN 1991-1-2; for each fire scenario the structural fire behaviour of entire structures, single members and various possible substructures is analyzed. The structural analyses are carried out by means of the non-linear software SAFIR2007 developed at the University of Liege, see Franssen 2008. The substructures are different for their limits and for the boundary conditions in order to highlight their influence on the assessment of the structural fire safety. Indeed, the choice of substructure, its limits and boundary conditions is not simple and it is depending on the fire scenario and the structural geometry, see Franssen 2005.

Some criteria, making easy the choice of the substructures which need to be analyzed for assessing the structural fire safety, are applied in the following for the designed steel-concrete frames (Nigro et al. 2009).

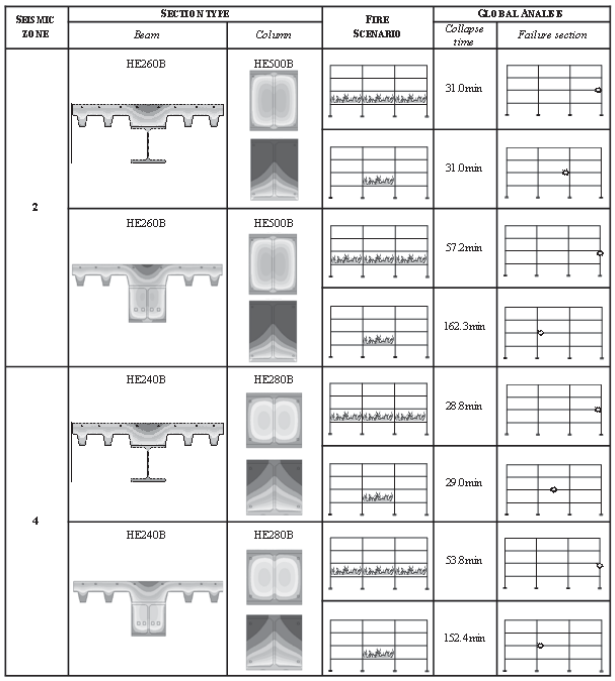

Figure 2.1.29. Global Analysis for the various kinds of designed frames subjected to fire.

In Figure 2.1.29 the global analysis results (collapse time, failure section) for two analyzed fire scenario are summarized: a) fire on the overall first floor; b) fire limited to the central span of the first floor. The comparison between the frames shows that the collapse time of the frame designed for seismic zone 4 is quite similar to those of the other frame, designed for seismic zone 2. This is a consequence of the internal forces' entity produced by constrained thermal expansions: those forces (named generally indirect effects) have a higher value for the frame designed for seismic zone 2, see Figure 2.1.29. Moreover, in the case of composite steel beam with partial concrete encasement the significant improvement of fire resistance time is remarked. In order to reduce the computational time, the substructure analysis can be used. However, the selection of a specific substructure affects the analysis' results. In Figure 2.1.30 is reported a comparison between the global and substructure analysis results (collapse time) for fire scenario 2. Meaningful is the case of b2 and c2 substructures subjected to fire scenario 2. The translational restraints in horizontal direction for nodes I and N allow a better development of the catenary action, see Usmani et al. 2001, along the heated beam. It produces an overestimation of the structure fire resistance time with respect to the global analysis results.

SEISMIC ZONE	GLOBAL ANALYSIS VS SUBSTRUCTURE ANALYSIS FIRE SCENARIO 2	BEAM SECTION TYPE	
			
2	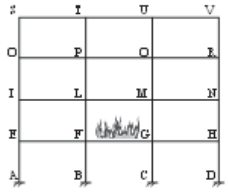 (a)	31.0 min	162.3 min
4		29.0 min	152.4 min
2	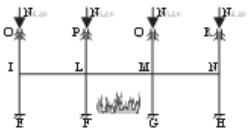 (b1)	31.8 min	162.2 min
4		30.0 min	157.0 min
2	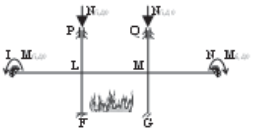 (b2)	33.0 min	167.0 min
4		36.5 min	>180.0 min
2	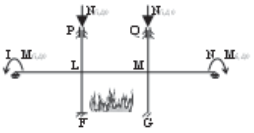 (b3)	31.0 min	158.0 min
4		27.0 min	127.0 min
2	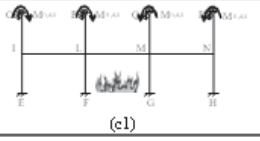 (c1)	32.0 min	162.0 min
4		29.2 min	150.2 min
2	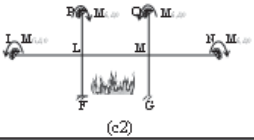 (c2)	33.5 min	169.0 min
4		37.5 min	>180.0 min
2	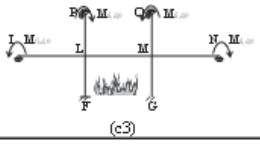 (c3)	31.0 min	156.0 min
4		29.5 min	134.0 min

Figure 2.1.30. Substructure Analysis results for fire scenario 2.

SEISMIC ZONE	SECTION TYPE		FIRE SCENARIO	GLOBAL ANALYSIS		SINGLE MEMBER ANALYSIS	
	Beam	*Column*		*Collapse time*	*Failure section*	*Collapse time*	*Failure section*
2	HE260B	HE500B	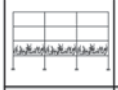	57.2 min	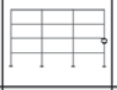	111 min	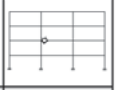
			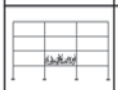	162.3 min	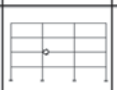	111 min	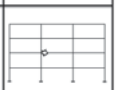
4	HE240B	HE280B	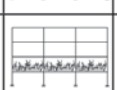	53.8 min	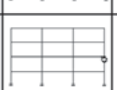	60 min	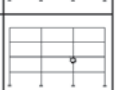
			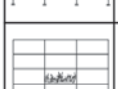	152.4 min	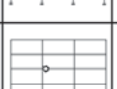	116 min	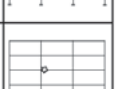

Figure 2.1.31. Single Member Analysis vs Global Analysis results.

The simplest substructure is the single member. Single member analysis allows considering the structures like an assembly of single elements (beams and columns): therefore, those analysis type does not allow to take account of the effects of the structural redundancy. In Figure 2.1.31 it is reported a comparison between the global and simple member analysis results (collapse time and failure section) for two fire scenario. The results of single member analysis are conservative when the element that collapse in the global analysis is a beam, because the catenary effect is neglected in the single member model. Instead, the single member analysis is not conservative when the element that collapses in the global analysis is a column, due to indirect actions produced by constrained thermal expansions.

2.1.8 FIRE RESISTANCE OF STRUCTURES AFTER EARTHQUAKE

2.1.8.1 State of the problem

The behaviour in fire of structures which have been damaged by earthquakes represents an important investigation field since in many cases fires break out after a seismic event, giving rise to a real catastrophe. In fact negative effects of fires on structures and human lives may be comparable to those of the earthquake itself. Moreover, even in case no fire develops immediately after an earthquake, the possibility of delayed fires affecting the structure must be adequately taken into account, since the earthquake induced damage makes the structure more vulnerable to fire effects than the undamaged one. This is because the consequence of fire on a structural system is mainly a gradual decay of the mechanical properties as far as temperature grows. It is apparent that the more the structural behaviour is degraded after an earthquake the more time up to collapse due to fire is short.

In view of the development of a comprehensive methodology of performance-based design of buildings, the fire resistance performance should be taken into account considering also the earthquake-induced damage for those buildings located in seismic areas. This consideration leads to the conclusion that the fire-safety codes should distinguish between structures located in seismic and non-seismic areas, by requiring more stringent fire resistance provisions for those buildings potentially subjected to seismic actions.

2.1.8.2Preliminary studies

In recent years, a number of studies on the behaviour of steel structures damaged by earthquakes and exposed to fires has been carried out (Della Corte et al. 2001, 2003a, b, 2005; Faggiano et al. 2005, Zaharia & Pintea, 2009). In particular some numerical analyses were devoted to investigate the effects of structural earthquake-induced damage on the fire resistance of MR steel frames. Modelling the behaviour of buildings subject to fires following earthquakes is a challenging but very difficult task for a structural engineer. In fact, not only knowledge about the mechanical response of the structure to the external action, but also dominance of several interdisciplinary issues, like modelling of seismic and fire actions is required. Grossly, the following general modelling aspects could be identified: a) modelling of the seismic action; b) modelling of the structural response during the earthquake; c) modelling of the fire action; d) modelling of the thermo-mechanical behaviour of the structure subject to fire.

A key aspect of the study has been the interpretation of the earthquake-induced damage, which has been done by means of a simple modelling scheme. In particular, structural damage has been schematised as the combination of two damage types: a ‘geometrical damage’, which consists of the residual deformation of the structure, and a ‘mechanical damage’, which consists of the reduction of the main mechanical properties of the structural components (stiffness and strength degradation). Figure 2.1.32 efficiently synthesises this scheme, evidencing that the structure after the earthquake could be subjected to significant residual P-Delta effects, which, together with the reduced lateral strength of the frame, could induce an important reduction of the frame fire resistance.

This schematisation allows for a rational evaluation of the mechanical state of the structure after the earthquake and of its mechanical behaviour under external actions succeeding the earthquake. In addition, it is a modelling very useful approach for parametrical analyses.

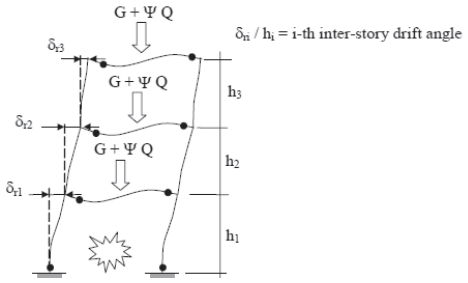

Figure 2.1.32. Residual P-Delta effects and local plastic deformation due to earthquake (Della Corte et al. 2005).

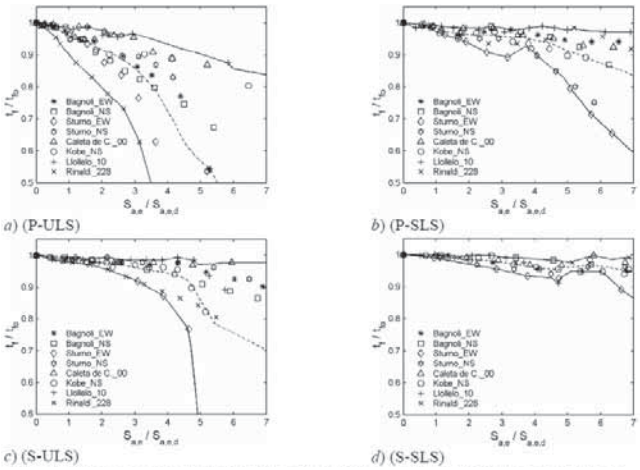

Figure 2.1.33. Fire resistance rating reductions of study MR steel frames subjected to earthquakes (Della Corte et al. 2005).

Figures 33a through 33d illustrate the normalized fire resistance rating reduction obtained for the four examined cases of MR steel frames (Perimeter and Spatial frames; designed at Ultimate Limit States, ULS, and Serviceability Limit State, SLS), as a function of the normalized spectral acceleration $S_{a,e}$, for a number of acceleration records.

The fire resistance rating reduction usually becomes non-negligible for very rare earthquakes, i.e. earthquakes having a mean return period larger than 475 years.

2.1.8.3 Refined approach

More comprehensive numerical simulations overcoming some conceptual and numerical limitations of the simplified models have been developed, preliminary to simple portal frames, in order to have a more accurate representation of seismic damage within the structure, see Faggiano et al., 2007a. At this aim, the finite element multi purpose computer program ABAQUS v.6.5 (2004) has been used, which allows to perform coupled thermal-displacement analyses, so giving the possibility to reproduce, in a step-by step process, the actual phases of the modelled phenomenon, from the application of the vertical loads and the earthquake induced damage up to the exposure of the structure to fire. Therefore the analysis procedure is articulated in three different phases:

1. Seismic analysis of structures;
2. Identification of the performance levels, according to the mentioned SEAOC indications;
3. Analysis under fire of the structures already damaged by earthquake, starting from each previously defined performance levels.

The seismic damaged states of the structures, characterizing the performance levels, are considered as initial configurations for the fire analysis, aiming at the evaluation of the effect of the seismic induced damage on the fire resistance and the collapse mode of the study structures.

2.1.9. FURTHER DEVELOPMENTS

Most of the current research work on structures subjected to elevated temperatures is dedicated to steel structures. The experimental and numerical studies show importance and complexity of beam to column connections in structural analysis Galambos (2000). The flexibility and strength of a connection pay important role in overall behaviour of many steel structures. At the same time the great variety of joint types require complex and unique analyses. The connections are also critical for the resistance of steel structures subjected to elevated temperatures, see Franssen & Zaharia (2006). Precise numerical analysis is complex as it should take into account many parameters such as contact between bolts, column flange, and end plate, stress concentration around bolts, prestressing forces. Material degradation and elongation caused by elevated temperature additionally complicates the study.

For concrete structures there are important and complex at the same time, thermo-hydro-mechanical phenomena resulting in nonlinear interaction among additional effects like transient creep strain, load induced thermal strain, shrinkage, pore pressures and spalling. The prediction of behaviour of concrete structures and structural elements imposes the main challenge for future research.

Another issue is the question about predictive capability for analysis of structures under fire, especially of the nonlinear global FE analysis intended to replicate real fires. The FEA model verification and validation is more often recognized as a procedure warranting modelling accuracy, see Oberkampf et al. 2004. The calculation verification is intended to estimate the numerical errors due to discrimination approximations. Validation, through mainly comparison with experiments, evaluates the accuracy with which the mathematical model depicts the actual physical event.

There is a need for experimental benchmark problems which could be used for the FE model validation. The test conditions in terms of loading, thermal and mechanical boundary conditions, and measurements should be clearly specified and easy to follow.

2.1.10 REFERENCES

Al-Jabria, K.S. Seibib, A. & Karrechc, A. 2006. Modelling of unstiffened flush end-plate bolted connections in fire. *Journal of Constructional Steel Research.* 62: 151–159.

Anderberg, Y. & Thelandersson, S. 1976. *Stress and Deformation Characteristic of Concrete at High Temperatures*, Part 2: Experimental Investigation and Material Behaviour Model. Bulletin 54. Lund: Lund University of Technology. 84 p.

ASM Specialty Handbook, 1993. Aluminium and aluminium alloys. Edited by J.R. Davis &Associates.

Bacinskas, D. Kaklauskas, G. & Gribniak, V. 2008. Layered section analysis of RC slabs subjected to fire, in *Proc. of the International fib Conference Fire Design of Concrete Structures*. Coimbra: University of Coimbra, 311–318.

Bratina, S. Saje, M. & Planinc, I. 2007. The effects of different strain contributions on the response of RC beams in fire, *Engineering Structures* 29(3): 418–430.

Capua Di, D. & Mari, A.R. 2007. Nonlinear analysis of reinforced concrete cross-sections exposed to fire, *Fire Safety Journal* 42(2): 139–149.

CEN, European Committee for Standardization, 2002. EN 1990 *Eurocode 0*: Basis of Structural Design. Brussels, Belgium.

CEN, European Committee for Standardization, 2002. 1991-1-2 *Eurocode 1*: Actions on structures – Part 1-2; General Actions – Actions on structures exposed to fire. Brussels, Belgium.

CEN, European Committee for Standardization, 2004a. *Eurocode 2*: Design of Concrete Structures – Part 1: General Rules and Rules for Buildings, EN 1992-1-1:2004. Brussels, Belgium.

CEN, European Committee for Standardization, 2004b. EN 1992-1-2, *Eurocode 3*: Design of concrete structures – Part 1-2: Structural fire design. Brussels, Belgium.

CEN, European Committee for Standardization, 2005a. EN 1993-1-2, *Eurocode 3*: Design of steel structures – Part 1-2: Structural fire design. Brussels, Belgium.

CEN, European Committee for Standardisation, 2005b. EN 1993-1-1, *Eurocode 3*, Design of Steel Structures – part 1-1. General rules and rules for buildings. Brussels, Belgium.

CEN, European Committee for Standardization, 2005c. EN 1994-1-2, *Eurocode 3*: Design of composite steel and concrete structures – Part 1-2: Structural fire design. Brussels, Belgium.

CEN, European Committee for Standardization, 2005d. prEN 1993-1-4, *Eurocode 3*: Design of steel structures – Part 1-4: Supplementary Rules for Stainless Steels. Brussels, Belgium.

CEN (European Communities for Standardisation), prEN 1999-1-2, 2003. Eurocode 9: Design of aluminium structures - Part 1-2: General rules-Structural fire design.. Brussels, Belgium.

Cervenka, J. Surovec, J. Fellinger, J. Feron, C. Wageneder, J. Kaklauskas G. & Corsi, F. 2005. FE Simulations of a Suspending Ceiling. Comparison of Fire Test Analyses, *UPTUN Report 441*, Brussels: UPTUN. 30 p.

Cooke, G.M.E. 2001. Behaviour of precast concrete floor slabs exposed to standardised fires, *Fire Safety Journal* 36(5): 459–475.

Della Corte G., Landolfo R., 2001. Post-earthquake fire resistance of steel structures, Safety and reliability, towards a safer World, Proceedings of the European Conference on Safety and Reliability – ESREL 2001, Torino, Italy.

Della Corte G., Landolfo R., Mammana O., 2003a. Fire resistance of MR frames damaged by earthquakes, Proceedings of the Fourth International Conference on the Behaviour of Steel Structures in Seismic Areas (STESSA 2003), Naples, Italy,.

Della Corte G., Landolfo R., Mazzolani F.M., 2003b. Post-earthquake fire resistance of moment-resisting frames, Fire Safety Journal, Vol. 38, pp. 593-612.

Della Corte G., Faggiano B., Mazzolani F.M., 2005. On the structural effects of the fire following earthquake, Proceedings of the Final Conference COST C12 "Improving buildings' structural quality by new technologies", Innsbruck, Austria.

ECCS. European Convention for Constructional Steelwork 1983. *European Recommendations for the Fire Safety of Steel Structures*. Elsevier.

ECCS. European Convention for Constructional Steelwork. 2006. *Rules for Member Stability in EN 1993-1-1:* Background documentation and Design Guidelines. ECCS publication no. 119, Brussels.

Faggiano B., De Matteis G., Landolfo R., Mazzolani F.M., 2003. On the behaviour of alluminium alloy structures exposed to fire. Proceedings of the XIX National Congress C.T.A. "III week of steel Constructions", 28-30 September, Genova, Italia, 393-406 pp..

Faggiano B., De Matteis G., Landolfo R., Mazzolani F.M., 2004a. The influence of material modelling on the fire resistance of aluminium alloy structures. Proceedings of the 9th International Conference on Aluminum Structural Design (INALCO 2004), Cleveland, Ohio (USA), 2-4 June.

Faggiano B., De Matteis G., Landolfo R., Mazzolani F.M., 2004b. Effects of high temperatures on the resistance of aluminium alloy structures. Proceedings of the 7th International Conference on Modern Building Materials, Structures and Techniques, Vilnius, Lithuania, 19-21 May.

Faggiano B., De Matteis G., Landolfo R., Mazzolani F.M. 2005a. "On the fire resistance of aluminium alloy structures". Proceedings of the Final Conference of the COST C12 "Improvement of buildings' structural quality by new technologies", Innsbruck, Austria, 20-22 January, A.A. Balkema Publishers, Taylor & Francis Group plc, London, UK, ISBN: 04-1536-609-7, pp. 267-275.

Faggiano B., Della Corte G., Mazzolani F.M., Landolfo R., 2005b. Post-earthquake fire resistance of moment resisting steel frames, Proceedings of the Eurosteel Conference on Steel and Composite Structures, Maastricht, The Neetherlands

Faggiano, B. Esposto, M. Mazzolani, F.M. 2007a. "Fully coupled temperature – displacement analyses of steel portal frames under fire". Atti del XXI Congresso CTA, Costruire con l'acciaio, Catania, Italia, a cura di A. Ghersi, Flaccovio Editore, ISBN 978-88-7758-787-9, pp. 561-568.

Faggiano B., Esposto M., Mazzolani F.M., Landolfo R., 2007b. Fire analysis on steel portal frames damaged after earthquake according to performance based design, COST Action C26 "Urban habitat constructions under catastrophic events", Proceedings of Workshop in Prague, pp. 35-40.

Franssen, J-M. 2005. SAFIR, A Thermal/Structural Program Modelling *Structures under Fire, Engineering Journal, A.I.S.C.*, Vol 42, No. 3, 143-158.

Franssen, J-M. & Zaharia, R. 2006. Design of Steel Structures Subjected to Fire: Background and Design Guide to Eurocode 3. *Fire Safety Journal*, *Volume 41, Issue 8*: 628-629.

Galambos, T.V. 2000. Recent research and design develop-ments in steel and composite steel–concrete structures in USA. *Journal of Constructional Steel Research*, Volume 55, Issues 1-3: 289-303.

Geda, E. 2010. Layer Model for Reinforced Concrete Members under Fire. *PhD dissertation*, Vilnius Gediminas Technical University, Vilnius, Lithuania. 118 p. (in Lithuanian).

Gribniak, V. Bacinskas, D. & Kaklauskas, G. 2006. Numerical simulation strategy of bearing RC tunnel members in fire, *The Baltic Journal of Road and Bridge Engineering* 1(1): 5–9.

Hajpál, M. 2000. Investigation of burnt sandstone, *Proceedings 1st international conference on Fire Protection of Cultural Heritage* 2000 Thessaloniki, pp 349-361.

Hajpál, M. & Török, Á. 2004. Physical and mineralogical changes in sandstones due to fire and heat. *Environmental Geology*, 46, 3, 306-312

Hajpál, M. 2008. Heat effect by natural stones used by historical monuments, *Proceedings 11th International Congress on Deterioration and Conservation of Stone* (STONE 2008).

Huang, Z. Burgess, I.W. & Plank, J.R. 1999. Nonlinear analysis of reinforced concrete slabs subjected to fire, *ACI Structural Journal* 96(1): 127–135.

Hallquist J.O. 2006. *LS-DYNA Keyword Manual*. Livermore: Livermore Software Technology Corporation.

Italian Technical Code for the Constructions 2008 (in Italian). "Norme Tecniche per le Costruzioni", Supplemento Ordinario della Gazzetta Ufficiale della Repubblica Italiana del 4 febbraio 2008, n. 29.

Kaklauskas, G. 2004. Flexural layered deformational model of reinforced concrete members, *Magazine of Concrete Research* 56(10): 575–584.

Kaklauskas, G. Bacinskas, D. Gribniak, V. & Geda, E. 2007. Mechanical simulation of reinforced concrete slabs subjected to fire, *Technological and Economic Development of Economy* 13(4): 295–302 (in Lithuanian).

Khennane, A.; Baker, G. 1993. Unaxial model for concrete under variable temperature and stress, *ASCE Journal Engineering Mechanics* 119(8): 1507–1525.

Khoury, G.A. 2000. Effect of Fire on Concrete and Concrete Structures. *Progress in Structural Engineering and Materials* 2(4): 429–447.

Kodur, V.K.R. & Dwaikat, M.B. 2008. A numerical model for predicting the fire resistance of reinforced concrete beams, *Cement and Concrete Composites* 30(5): 431–443.

Kosiorek, M. 2002. Fire safety in regulations and designing; *Fire Protection*, 1/2002 (1).

König, J. 2005. Structural fire design according to Eurocode 5-design rules and their background. *Fire and materials* 29:147–163 Wiley InterScience.

Nielsen, C.V. Pearce C. J. & Bicanic N. 2004. Improved Phenomenological Modelling of Transient Thermal Strains for Concrete at High Temperatures. *Computers and Concrete* 1(2): 189–209.

Nigro E., Ferraro A., Cefarelli G. 2008. Structural fire analysis of composite steel and concrete frames (in Italian), Costruzioni Metalliche, n. 6, December 2008, ACAI, pp. 51-64.

Nigro E., Pustorino S., Cefarelli G., Princi P. 2009. Progettazione di strutture in acciaio e composte acciaio-calcestruzzo in caso di incendio, Ed. Hoepli, Milano.

Oberkampf, W.L. Trucano, T.G. & Hirsch C. 2004. Verification, validation, and predictive capability in computational engineering and physics, *Appl. Mech. Rev.* 57 (5), 345–384.

Shapiro, A. 2005. Heat Transfer in LS-DYNA, *5th European LS-DYNA Users Conference New Applications and Developments*, Birmingham, UK.

Schneider, U. & Horvath, J. 2003. *Behaviour of Ordinary Concrete at High Temperatures.* Research Report, Vol. 9. Institute for Building Materials, Buildings Physics and Fire Protection, Vienna University of Technology.

SCI, Steel Construction Institute. 1996. Structural Fire Design to EC3 & EC4, and comparison wit5h BS 5950. *Technical Report*, SCI publication no. 159.

Terro, M.J. 1998. Numerical modeling of the behavior of concrete structures in fire, *ACI Structural Journal* 95(2): 183–193.

Török, Á. & Hajpál, M. 2005. Effect of Temperature Changes on the Mineralogy and Physical properties of Sandstones. A Laboratory Study. *International Journal for Restoration of Buildings and Monuments*, 11, 4, Freiburg, 211-217.

Tybura, A. & Kwaśniewski, L. (2008) Computer Simulation of the Steel Connection at Elevated Temperatures, *Proceedings of XIII Slovak - Polish - Russian seminar Theoretical Foundation of Civil Engineering,* MGSU, Moscow, Russia, Warszawa-Wroclaw, Poland, 02-06.06.2008, pp. 231-236.

Usmani A.S., Rotter J.M., Lamont S., Sanad A.M., Gollie M. 2001. Fundamental Principles of Structural Behaviour Under Thermal Effects. Fire Safety, 2001(36): 721-724.

Vila Real, P.M.M. & Franssen, J.-M. 2010. Elefir-EN, http:// elefiren.web.ua.pt.

Wang, Y.C. 1997. The effects of frame continuity on the behaviour of steel c columns under FIRE conditions and FIRE resistant design proposals, *J. Construct. Steel Res*., Vol. 41, No. 1, pp. 93-111.

Youssef, M.A. & Moftah, M. 2007. General Stress–Strain Relationship for Concrete at Elevated Temperatures. *Engineering Structures* 29(3): 2618–2634.

Xiao, J. & Konig, G. 2004. Study on concrete at high temperature in China an overview, *Fire Safety Journal* 39(1): 89–103.

Zaharia, R. & Pintea, D., Fire after earthquake analysis of steel moment resisting frames, *International Journal of Steel Structures,* December 2009, Vol 9, No 4, 275-284